Journal of Nuclear Medicine, published on October 23, 2020 as doi:10.2967/jnumed.120.252783

Principal components analysis based measures of PET data closely reflect neuropathological staging schemes

Ganna Blazhenets[†], MSc, Lars Frings, PhD, Arnd Sörensen, PhD, and Philipp T. Meyer, MD, PhD, for the Alzheimer's Disease Neuroimaging Initiative*

†corresponding author

Department of Nuclear Medicine, Medical Center – University of Freiburg, Faculty of Medicine, University of Freiburg, Freiburg, 79106, Germany

Short title: PET reflects neuropathological staging

Disclosure: The authors declare they did not receive any funding for this study. PTM received honoraria from GE (presentation, consultancy) and Philips (presentation). All declared interests are outside of the submitted work.

Word count: 4267

Corresponding Author: G. Blazhenets, Hugstetter Str. 55, 79106, Freiburg, Germany.

ganna.blazhenets@uniklinik-freiburg.de , Tel: +0049 761 270 38861.

ORCID ID: 0000-0003-2419-7373

ABSTRACT

Voxel-based principal components analysis allows for an identification of patterns of glucose metabolism and amyloid deposition related to the conversion from mild cognitive impairment (MCI) to Alzheimer's dementia (ADCRP). Present study aimed to validate these ADCRPs against neuropathological findings.

Methods We included patients from the Alzheimer's disease (AD) neuroimaging initiative who underwent autopsy and for whom ^{18}F-FDG [30 AD dementia, 6 MCI, 2 cognitively normal (CN)] and amyloid-beta (Aβ) [17 AD dementia, 3 MCI, 2 CN] PET were available. Pattern expression scores (PES) of the FDG- and Aβ-ADCRP were compared to Braak tangle stage and Thal amyloid phase, respectively. Mean ^{18}F-FDG uptake and mean ^{18}F-AV-45 standardized uptake value ratio (SUVr) in regions of hypometabolism and elevated amyloid load typical for AD, respectively, were employed as volume of interest (VOI)-based PET measures. The diagnostic performance for identifying none-to-low vs. intermediate-to-high AD neuropathological change (ADNC) was assessed for all biomarkers.

Results We observed significant associations between PES of FDG-ADCRP and Braak stage ($\rho>0.48$, $P<0.005$) and between PES of Aβ-ADCRP and Thal phase ($\rho>0.66$, $P<0.001$). PES of FDG-ADCRP, PES of Aβ-ADCRP, and their combination identified intermediate-to-high ADNC with an area under receiver operating characteristic curve (AUC) of 0.80, 0.95, and 0.98 (n=22), respectively. Mean ^{18}F-FDG uptake and mean ^{18}F-AV-45 SUVr in AD-typical regions were also significantly associated with Braak stage ($|\rho|>0.45$, $P<0.01$) and Thal phase ($\rho>0.55$, $P<0.01$), respectively. VOI-based PET measures discriminated between ADNC stages with an AUC of 0.79, 0.88, and 0.90, for mean ^{18}F-FDG uptake, mean ^{18}F-AV-45 SUVr, and their combination (n=22), respectively. Contemplating all subjects with available ^{18}F-FDG PET/neuropathology information (n=38), PES of FDG-ADCRP was a significant predictor of intermediate-to-high ADNC (AUC=0.72), while mean ^{18}F-FDG uptake was not (AUC=0.66), albeit the difference between methods was not significant.

Conclusion PES of FDG-ADCRP, a measure of neurodegeneration, shows close correspondence with the extent of tau pathology, as assessed by Braak tangle stage. PES of Aβ-ADCRP is a valid biomarker of

underlying amyloid pathology, as demonstrated by its strong correlation with Thal phase. The combination of ADCRPs performed superior to FDG-ADCRP alone, albeit there was only negligible improvement compared to Aβ-ADCRP.

Keywords: ^{18}F-FDG PET, amyloid PET, Braak tangle stage, Thal phase, conversion pattern.

INTRODUCTION

A definite diagnosis of Alzheimer's disease (AD) requires autopsy and neuropathological assessment (*1*). According to the National Institute on Aging and the Alzheimer's Association guidelines for the neuropathological assessment of AD, the presence of neurofibrillary tangles (NFTs) and neuritic plaques are considered essential for the AD diagnosis (*2*). The recently introduced AT(N) classification scheme (*3*) shifted the diagnostic landscape from clinical symptomatology towards *in vivo* biomarkers for lifetime diagnosis of AD. Still, the gold standard, against which *in vivo* assessments must be validated, is neuropathological examination.

There are only a limited number of studies that assessed the quantitative relationship between the AD pathology and ante-mortem PET imaging (*4-7*). We recently applied principal components analysis (PCA) to amyloid-beta (Aβ) and ^{18}F-FDG PET data to identify the AD dementia conversion-related patterns of regional glucose metabolism (FDG-ADCRP) and amyloid load (Aβ-ADCRP), which significantly predict conversion to AD dementia in patients with mild cognitive impairment (MCI) (*8,9*). Thus, the incorporation of ADCRPs into research diagnostic criteria may allow identifying high-risk individuals already at prodromal stages of the disease. For further validation, the confirmation with neuropathology data is of high importance. Therefore, we investigated the relationship between FDG- and Aβ-ADCRP and neuropathology findings as expressed by Braak stage of NFTs (*10*) and Thal amyloid phase for neuritic plaques (*11*), respectively, and the value of individual and combined measures to identify the AD neuropathological change (ADNC) stages (*12*).

MATERIALS AND METHODS

Patient Cohort

As of October 2019, a total of 64 patients from the AD neuroimaging initiative (ADNI, ClinicalTrials.gov Identifier: NCT00106899, www.adni-info.org) underwent autopsy. For this analysis, we included 38 patients with available ^{18}F-FDG PET data (Age [mean ± SD]: 79±8 years; all male). 30 patients were clinically diagnosed with AD dementia, 6 with MCI, and 2 were cognitively unimpaired (CN) participants. Additionally, for 22 of these patients ^{18}F-AV-45 amyloid PET data were present (17 AD dementia, 3 MCI, and 2 CN). For the majority of patients, PET imaging was performed within two years prior the autopsy (^{18}F-FDG PET, N = 21/38; amyloid PET, N= 12/22). Mini-mental state examination (MMSE) score significantly differed between diagnostic groups, while gender, age, and years of education were matched between groups. Ante mortem imaging, demographic, and clinical information of patients was downloaded from ADNI database (Table 1). The study protocol was approved by ADNI Institutional Review Board and written informed consent had been obtained by ADNI from all subjects before protocol-specific procedures were carried out (see ADNI protocols).

Neuroimaging

PET acquisitions and data preprocessing were performed as previously described (*8*). For ^{18}F-FDG PET (acquired 30 to 60 minutes p. i.), we assessed the pattern expression score (PES) of the previously validated FDG-ADCRP (*8*), which was constructed by voxel-wise PCA (*13*). The FDG-ADCRP is characterized by the most prominent decreases of metabolism in the bilateral temporoparietal cortex as well as the precuneus/posterior cingulate cortex, while the metabolism of the sensorimotor and occipital cortices and cerebellum is relatively increased (preserved) (Supplemental Figure 1A). Similarly, for ^{18}F-AV-45 PET (acquired 50 to 70 minutes p. i.) the PES of the Aβ-ADCRP (*9*) was obtained by PCA on the amyloid PET data. The Aβ-ADCRP is characterized by the most prominently elevated amyloid load in the bilateral precuneus, posterior cingulate cortex, the mesial frontal cortex, the insular region and ventral striatum, while the cerebellum is spared (Supplemental Figure 1B). Additionally, volume of

interest (VOI)-based measures of cerebral ^{18}F-FDG uptake and ^{18}F-AV-45 Aβ binding were used. Mean normalized ^{18}F-FDG uptake was calculated in regions of significant hypometabolism in MCI subjects who converted to AD dementia compared to stable MCI subjects (obtained from a voxel-wise two-sampled *t*-test performed in a previous study (*8*)). These regions comprised bilateral temporoparietal regions and the precuneus/posterior cingulate cortex (see Supplemental Figure 1C). Mean standardized uptake value ratio (SUVr) of ^{18}F-AV-45 in regions with the highest beta-amyloid burden in AD (*14*) (bilateral middle frontal, middle occipital, temporal and superior parietal regions; cerebellar cortex as reference, Supplemental Figure 1D) was used as VOI-based Aβ PET measure.

Neuropathology

Autopsies were performed at participating centers according to the established neuropathological procedures (*15*). Formalin-fixed paraffin embedded brain tissue blocks were sent to the ADNI Neuropathology Core for analysis. The diagnosis was established following the criteria for the pathological diagnosis of AD (*16*). Braak NFTs stage (*10*), Thal amyloid phase (*11*), and ADNC (*12*) were selected for comparison to neuroimaging data.

Statistical Analyses

The relationship between neuroimaging biomarkers (PCA- and VOI-based) among each other and with neuropathological schemes was assessed with Spearman's correlation coefficients (zero order correlation). To account for the delay from PET examination to death (scan-to-death time), the partial Spearman's correlation between neuroimaging and neuropathology data was calculated while controlling for the scan-to-death time (partial correlation).

To explore possible additive value of combining biomarkers in predicting none-to-low vs. intermediate-to-high ADNC stage, we used logistic regressions to construct optimal combinations of biomarkers (separately for PCA- and VOI-based biomarkers). The diagnostic performance of PCA- and VOI-based biomarkers and their combinations (weighting defined by logistic regression) for classifying

between none-to-low vs. intermediate-to-high ADNC stages was assessed and compared by receiver operating characteristic (ROC) analyses and the DeLong test (*17*). The optimal cut-off points were defined based on Youden's index criterion and respective values for sensitivity and specificity were calculated. Of note, we did not correct for scan-to-death time as a covariate, as the effect of this covariate was small and only inconsistently observed. All statistical analyses were conducted in R (*18*) and MedCalc (Version 12.7.8.0).

RESULTS

PES of ADCRP vs. NFT and Aβ stages

We observed a significant association between PES of FDG-ADCRP and Braak stages of NFTs ($\rho = 0.48$, $P = 0.002$, Figure 1A). This relationship was slightly strengthened by taking into account scan-to-death time ($\rho = 0.50$, $P = 0.001$).

The PES of Aβ-ADCRP was significantly correlated with the Thal amyloid phase ($\rho = 0.66$, $P = 8\times10^{-4}$, Figure 1B). This correlation was slightly stronger when accounting for scan-to-death time ($\rho = 0.71$, $P = 3\times10^{-4}$).

VOI-based Measures vs. NFT and Aβ stages

Mean normalized ^{18}F-FDG uptake in regions of AD-typical hypometabolism showed a moderate association with the PES of FDG-ADCRP ($\rho = -0.64$, $P = 2\times10^{-5}$). Mean normalized ^{18}F-FDG uptake in regions of AD-typical hypometabolism was also significantly associated with Braak stage ($\rho = -0.45$, $P = 0.005$, Figure 1C). The relationship between measures was not strengthened when we also accounted for the scan-to-death time ($\rho = -0.45$, $P = 0.005$).

Mean SUVr in AD-typical regions as derived from ^{18}F-AV-45 PET was strongly correlated with PES of Aβ-ADCRP ($\rho = 0.86$, $P = 1\times10^{-6}$). Mean SUVr was significantly associated with the Thal phase ($\rho = 0.55$, $P = 0.008$, Figure 1D). Albeit these association were slightly improved when scan-to-death time was taken into account ($\rho = 0.58$, $P = 0.006$), the correlations between PES of Aβ-ADCRP and pathology (see above: $\rho = 0.71$) remained slightly higher.

Prediction of AD Pathology

PCA-based measures: Logistic regression was used to establish a diagnostically optimal combination of the PES of FDG- and Aβ-ADCRPs to predict none-to-low vs. intermediate-to-high ADNC (combined score = 0.11×PES of FDG-ADCRP + 0.20×PES of Aβ-ADCRP – 1.62; yielding 95% correct predictions). The combined PES score exhibited a moderate to strong correlation with the 4-step ADNC

score (ρ = 0.73, *P* = 0.0001, see Figure 2A), which was not improved when accounting for the scan-to-death time (ρ = 0.73, *P* = 0.0001). PES of FDG- and Aβ-ADCRPs and their combination were significant predictors of none-to-low vs. intermediate-to-high ADNC stage with ROC AUC of 0.80 (0.72 in all available ^{18}F-FDG PET/neuropathology datasets, n = 38), 0.95 and 0.98, respectively (see details including cut-offs, sensitivity and specificity in Table 2 and Figure 3A). The combined PES yielded a significantly higher ROC AUC than PES of FDG-ADCRP (*P* = 0.04; n = 22 overlapping datasets), while the differences between the PES of FDG- and Aβ-ADCRPs and between the PES of Aβ-ADCRP and the combined PES score was not significant (*P* = 0.13 and *P* = 0.25, respectively).

VOI-based measures: The optimal combination of VOI-based mean normalized ^{18}F-FDG uptake and mean SUVr in AD-typical regions to predict none-to-low vs. intermediate-to-high ADNC was: combined score = -13.75× mean ^{18}F-FDG uptake + 8.63× mean ^{18}F-AV-45 SUVr + 3.58 (91% correct predictions). The combined VOI-based measure showed a moderate correlation with the 4-step ADNC score (ρ = 0.62, *P* = 0.002, Figure 2B), which was not improved when accounting for the scan-to-death time (ρ = 0.62, *P* = 0.002). Mean ^{18}F-AV-45 SUVr and the combined VOI-based measure were significant predictors of none-to-low vs. intermediate-to-high ADNC (ROC AUC of 0.88 and 0.90, respectively), while the predictive value of mean normalized ^{18}F-FDG uptake in AD-typical regions was only different from chance (ROC AUC = 0.50) when the restricted dataset (n = 22; ROC AUC = 0.79) but not all available FDG PET/neuropathology datasets (n = 38; AUC = 0.66) were contemplated (see Table 2, Figure 3B-C). Differences in ROC AUC between single and combined VOI-based measures were not significant (all *P* > 0.17).

Likewise, exploratory pairwise comparison of the ROC AUC between overlapping (n = 22) ^{18}F-FDG PET, Aβ PET, and combined measures yielded no significant differences (all *P* > 0.2). Cases that were misclassified by both methods (VOI- and PCA-based) are summarized in Supplemental Table 1.

DISCUSSION

The PES of FDG-ADCRP and the PES of Aβ-ADCRP have previously proven their usefulness in the prediction of conversion from MCI to AD dementia (*8,9*). In this study, we compare these PCA-based PET biomarkers to neuropathological data in patients who underwent autopsy. We demonstrate significant associations between PET data (PES of FDG-ADCRP and PES of Aβ-ADCRP) and neuropathological findings (Braak stage and Thal phase, respectively). Furthermore, a combination of PES of FDG- and Aβ-ADCRPs showed a moderate to strong correlation with ADNC and was highly accurate in predicting intermediate-to-high ADNC stages. Further exploratory analyses suggest that the combined PES of FDG- and Aβ-ADCRP is superior predictor compared to FDG-ADCRP alone but only marginally better than Aβ-ADCRP (n = 22 with FDG- and Aβ-PET). These analyses yielded no significant differences between PCA- and VOI-based methods. However, PES of FDG-ADCRP was a significant predictor of intermediate-to-high ADNC stages, while mean ^{18}F-FDG uptake was not when contemplating all subjects with available ^{18}F-FDG PET/neuropathology information (n = 38).

The delay from scan to death and autopsy may crucially affect the relationship of PET measures with neuropathology. This is particularly true for biomarkers of ongoing neurodegeneration, while amyloid accumulation decelerates during the dementia phase of AD (*19*). Thus, the scan-to-death delay was included in the analyses as some patients underwent an autopsy more than two years after ^{18}F-FDG PET which may bias the results towards relatively weaker neurodegeneration on ^{18}F-FDG PET. However, this correction had only little effect. Neurodegeneration is not a direct measure of the Braak stage of neurofibrillary tangles, even though it closely reflects the latter (*20*). Likewise, ^{18}F-FDG PET as a marker of neurodegeneration (*3*) only indirectly reflects tau pathology assessed by ADNC. In contrast, amyloid PET directly reflects Thal phases (*21*). This may well explain why amyloid PET provides a considerably better prediction of none-to-love vs. intermediate-to-high ADNC stages and the actual benefit of adding ^{18}F-FDG PET is small. The present results are also in a good agreement with the study of La Joie et al. (*6*) in which intermediate-to-high ADNC was predicted by ^{11}C-Pittsburg compound B PET (Centiloid measure; n = 179 patients) with an ROC AUC of 0.90.

Although we primarily investigated the value of PCA as an advanced method for the PET data analysis, conventional measures based on preselected VOIs that are frequently used in clinical and research settings were also evaluated. PCA applied to amyloid PET data led to some improvement of the relationship between amyloid PET and neuropathological staging (ρ = 0.66-0.71, without and with correction for scan-to-death time) compared to conventional amyloid PET analysis (ρ = 0.55-0.58) and the ability to predict intermediate-to-high ADNC stages (ROC AUC = 0.95 vs. 0.88), albeit this difference failed to reach statistical significance in the present small study cohort.

Likewise, overall correlation between the mean ^{18}F-FDG uptake in regions with AD-typical hypometabolism and Braak tangle stage (ρ = -0.45) was slightly weaker in comparison to the PES of FDG-ADCRP (ρ = 0.48-0.50). Despite different VOIs and reference region used in our study, the correlation between mean normalized ^{18}F-FDG uptake in regions of AD-typical hypometabolism and Braak tangle stage was similar to the correlation reported by Lowe et al. (*4*) (ρ = -0.36 to -0.45). For amyloid PET measures, we observed a slightly weaker correlation to Thal phase in comparison to that study using Pittsburgh compound B PET (ρ = 0.55-0.58 for mean SUVR and ρ = 0.66-0.71 for PES of Aβ-ADCRP vs. ρ = 0.75-0.76 in Lowe et al. (*4*)), which might be explained by methodological factors (e.g., different PET tracers, multiple sites/scanners in case of ADNI data) and the much smaller cohort (n = 22 vs. n = 100), among other factors.

Of note, not all subjects suffered from dementia and AD in case of dementia (see Table 1). We did not exclude cases with non-AD diagnosis (n = 6/38) to reflect the clinical situation and estimate specificity. This allowed us to contemplate a wider range of neuropathological changes for validation of PET measures. However, the study is still limited by the overall low number of cases (including cases without pathology) and the distribution of Thal phase in present cohort was biased towards low- and high-phases with no intermediate-range diagnosis present. Thus, particularly the comparison between analysis methods has to be viewed as preliminary, warranting further evaluation in larger datasets.

CONCLUSION

PES of FDG-ADCRP, a measure of neuronal injury and neurodegeneration, shows a close correspondence with the extent of tau pathology, as assessed by Braak tangle stage. PES of Aβ-ADCRP is a valid biomarker of underlying amyloid pathology, as demonstrated by its strong correlation with Thal amyloid phase. The combined score of FDG- and Aβ-ADCRP performed superior to FDG-ADCRP alone in predicting intermediate-to-high ADNC stages, albeit there was only negligible improvement compared to Aβ-ADCRP. Further studies of sufficient sample sizes are needed to explore possible performance differences between PCA- and VOI-based methods.

ACKNOWLEDGEMENTS

Data collection and sharing for this project was funded by the Alzheimer's Disease Neuroimaging Initiative (ADNI) (National Institutes of Health Grant U01 AG024904) and DOD ADNI (Department of Defense award number W81XWH-12-2-0012).

KEY POINTS

QUESTION: Do advanced methods of PET data evaluation reflect neuropathological staging schemes, and if so, do they perform better than conventional methods of PET data evaluation?

PERTINENT FINDINGS In this cohort study, Alzheimer's dementia conversion-related patterns of regional glucose metabolism (FDG-ADCRP) and amyloid load (Aβ-ADCRP) significantly correlate with Braak tangle stage ($\rho > 0.48$) and Thal amyloid phase ($\rho > 0.66$) and allow for predicting severe Alzheimer's disease neuropathological changes (ADNC) with high ROC AUC of 0.80 and 0.95, respectively. VOI-based measures of ^{18}F-FDG and amyloid PET were also significantly associated with Braak stage ($|\rho| > 0.45$) and Thal phase ($\rho > 0.55$), and discriminated between ADNC stages with an ROC AUC of 0.79 and 0.88, respectively.

IMPLICATIONS FOR PATIENT CARE These results are of high relevance by opening the opportunity to accurately predict underlying AD pathology based on the PET measures.

REFERENCES

1. McKhann G, Drachman D, Folstein M, Katzman R, Price D, Stadlan EM. Clinical diagnosis of Alzheimer's disease: report of the NINCDS-ADRDA Work Group under the auspices of Department of Health and Human Services Task Force on Alzheimer's Disease. *Neurology.* 1984;34:939-944.

2. Hyman BT, Phelps CH, Beach TG, et al. National Institute on Aging-Alzheimer's Association guidelines for the neuropathologic assessment of Alzheimer's disease. *Alzheimers Dement.* 2012;8:1-13.

3. Jack CR, Jr., Bennett DA, Blennow K, et al. NIA-AA Research Framework: Toward a biological definition of Alzheimer's disease. *Alzheimers Dement.* 2018;14:535-562.

4. Lowe VJ, Lundt ES, Albertson SM, et al. Neuroimaging correlates with neuropathologic schemes in neurodegenerative disease. *Alzheimers Dement.* 2019;15:927-939.

5. Toledo JB, Cairns NJ, Da X, et al. Clinical and multimodal biomarker correlates of ADNI neuropathological findings. *Acta Neuropathol Commun.* 2013;1:65.

6. La Joie R, Ayakta N, Seeley WW, et al. Multisite study of the relationships between antemortem [(11)C]PIB-PET Centiloid values and postmortem measures of Alzheimer's disease neuropathology. *Alzheimers Dement.* 2019;15:205-216.

7. Thal DR, Ronisz A, Tousseyn T, et al. Different aspects of Alzheimer's disease-related amyloid beta-peptide pathology and their relationship to amyloid positron emission tomography imaging and dementia. *Acta Neuropathol Commun.* 2019;7:178.

8. Blazhenets G, Ma Y, Sorensen A, et al. Principal components analysis of brain metabolism predicts development of Alzheimer dementia. *J Nucl Med.* 2019;60:837-843.

9. Blazhenets G, Ma Y, Sorensen A, et al. Predictive value of (18)F-Florbetapir and (18)F-FDG PET for conversion from mild cognitive impairment to Alzheimer dementia. *J Nucl Med.* 2020;61:597-603.

10. Braak H, Braak E. Neuropathological stageing of Alzheimer-related changes. *Acta Neuropathol.* 1991;82:239-259.

11. Thal DR, Rub U, Orantes M, Braak H. Phases of A beta-deposition in the human brain and its relevance for the development of AD. *Neurology.* 2002;58:1791-1800.

12. Montine TJ, Phelps CH, Beach TG, et al. National Institute on Aging-Alzheimer's Association guidelines for the neuropathologic assessment of Alzheimer's disease: a practical approach. *Acta Neuropathol.* 2012;123:1-11.

13. Eidelberg D. Metabolic brain networks in neurodegenerative disorders: a functional imaging approach. *Trends Neurosci.* 2009;32:548-557.

14. Frings L, Hellwig S, Spehl TS, et al. Asymmetries of amyloid-beta burden and neuronal dysfunction are positively correlated in Alzheimer's disease. *Brain.* 2015;138:3089-3099.

15. Cairns NJ, Taylor-Reinwald L, Morris JC, Alzheimer's Disease Neuroimaging I. Autopsy consent, brain collection, and standardized neuropathologic assessment of ADNI participants: the essential role of the neuropathology core. *Alzheimers Dement.* 2010;6:274-279.

16. Consensus recommendations for the postmortem diagnosis of Alzheimer's disease. The National Institute on Aging, and Reagan Institute Working Group on diagnostic criteria for the neuropathological assessment of Alzheimer's disease. *Neurobiol Aging.* 1997;18:S1-2.

17. DeLong ER, DeLong DM, Clarke-Pearson DL. Comparing the areas under two or more correlated receiver operating characteristic curves: a nonparametric approach. *Biometrics.* 1988;44:837-845.

18. *R: A Language and Environment for Statistical Computing* [computer program]. Version: R Foundation for Statistical Computing; 2019.

19. Jack CR, Jr., Knopman DS, Jagust WJ, et al. Hypothetical model of dynamic biomarkers of the Alzheimer's pathological cascade. *Lancet Neurol.* 2010;9:119-128.

20. Nelson PT, Alafuzoff I, Bigio EH, et al. Correlation of Alzheimer disease neuropathologic changes with cognitive status: a review of the literature. *J Neuropathol Exp Neurol.* 2012;71:362-381.

21. Murray ME, Lowe VJ, Graff-Radford NR, et al. Clinicopathologic and 11C-Pittsburgh compound B implications of Thal amyloid phase across the Alzheimer's disease spectrum. *Brain.* 2015;138:1370-1381.

FIGURES

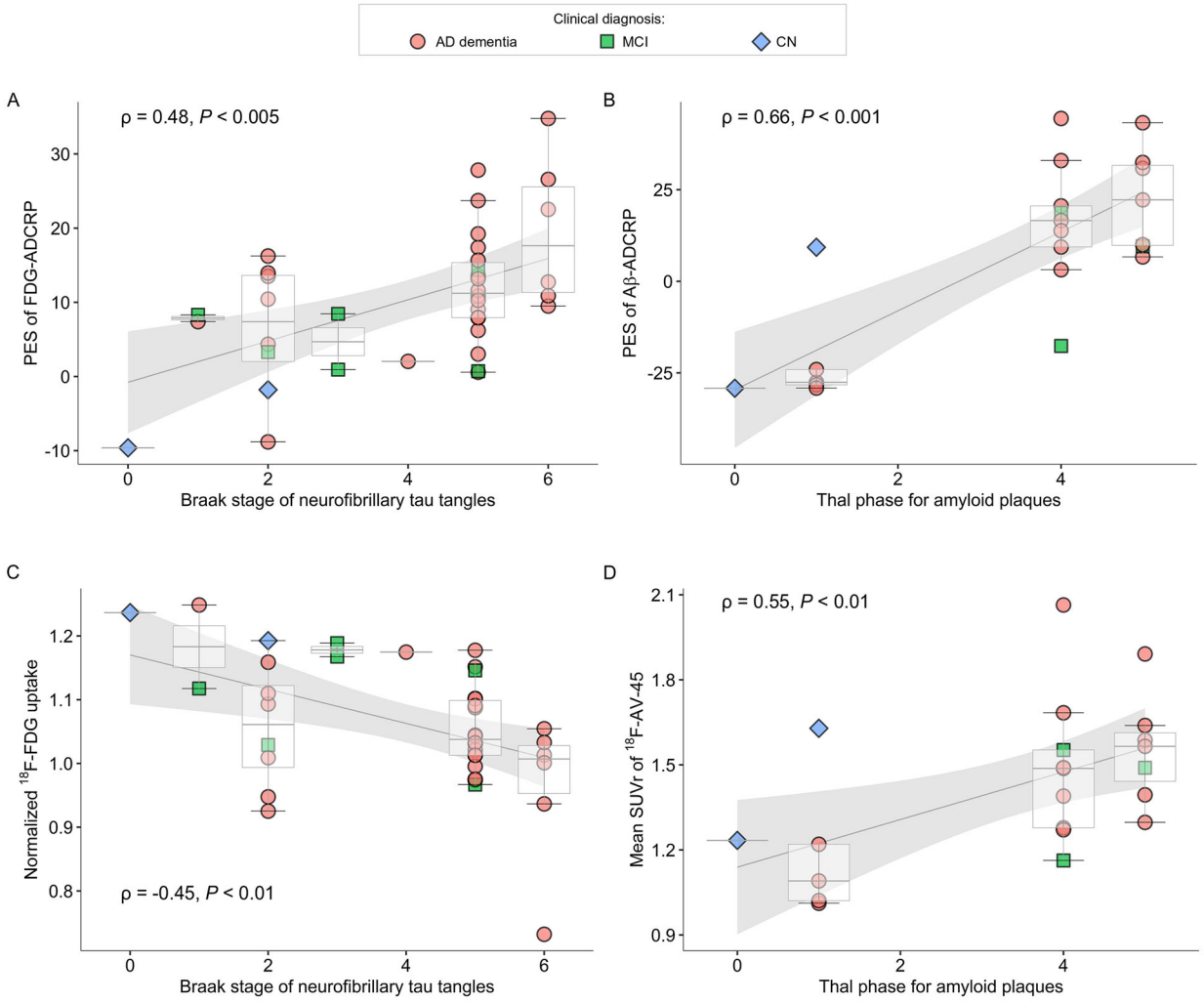

FIGURE 1. Associations between PET measures and neuropathology. Associations between PCA-based Alzheimer's dementia conversion-related patterns (ADCRP) and neuropathological stages: PES of FDG-ADCRP and Braak stage of tau tangles (A), and the PES of Aβ-ADCRP and Thal phase of amyloid plaques (B). Association between VOI-based measures and neuropathological stages: mean normalized ^{18}F-FDG uptake and Braak stage of neurofibrillary tau tangles (C) and mean SUVr of ^{18}F-AV-45 and Thal phase of Aβ plaques (D). The Spearman's correlation coefficients and *P*-values reflect the strength and significance of association between variables.

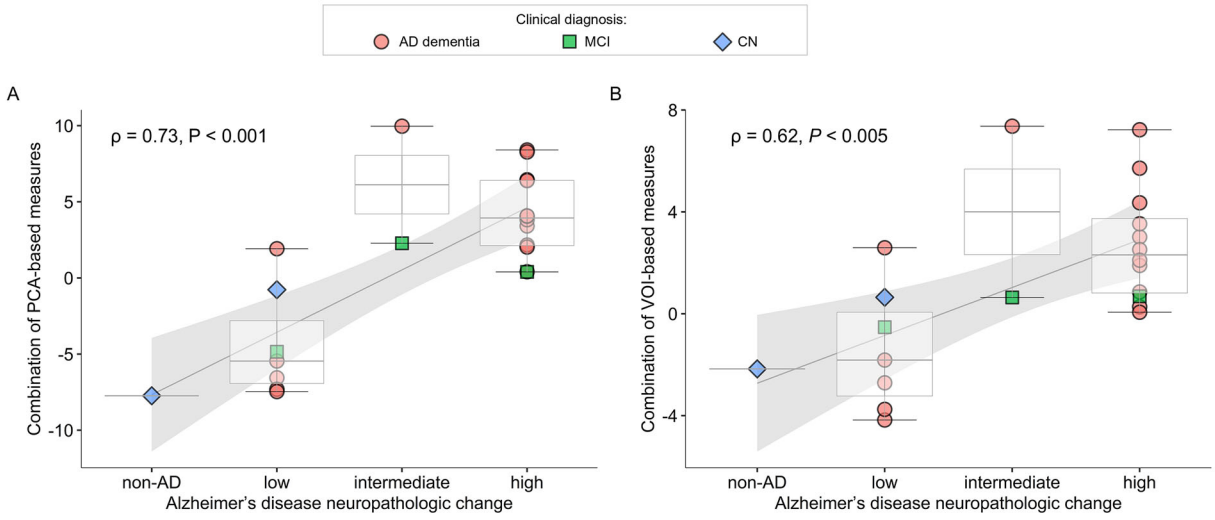

FIGURE 2. Associations between combinations of ^{18}F-FDG and amyloid PET measures and Alzheimer's disease neuropathological changes. The respective associations are shown for a combination of PCA-based (A) and VOI-based (B) measures. Spearman's correlation coefficients and *P*-values reflect the strength and significance of association between variables.

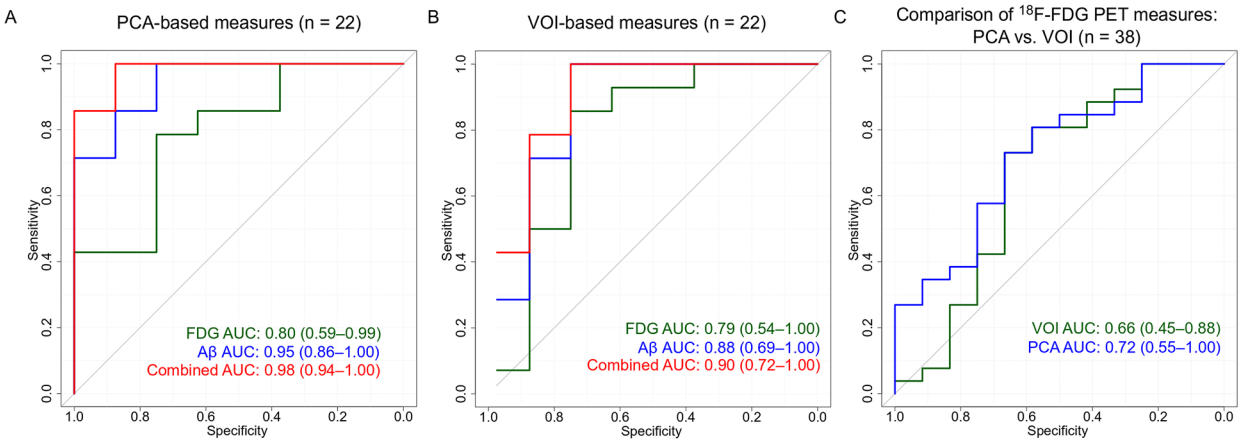

FIGURE 3. Receiver-operating characteristic (ROC) analyses for classifying between none-to-low vs. intermediate-to-high Alzheimer's disease neuropathological changes. The areas under the ROC curves (AUC) are given for the respective ^{18}F-FDG PET, Aβ PET, and combined outcome measures for PCA-based (A) and VOI-based (B) biomarkers (for n = 22 patients). The comparison between PCA- and VOI-based ^{18}F-FDG PET measures when contemplating all subjects with available ^{18}F-FDG PET/neuropathology information (n = 38).

TABLES

TABLE 1. Demographic characteristics of the ADNI sub-cohort with available neuropathology data according to the *ante mortem* clinical diagnostic groups.

Clinical diagnosis	**AD dementia**	**Mild cognitive impairment**	**Cognitively normal**
Subjects with ^{18}F-FDG PET available			
Number of subjects	30	6	2
Age at scan [mean ± SD]	79.2 ± 8.0	82.7 ± 6.0	76.1 ± 13.6
Age at autopsy [mean ± SD]	82.1 ± 8.1	85.0 ± 5.0	79.5 ± 13.4
Scan-deaths, years [mean ± SD]	2.9 ± 1.7	2.1 ± 1.4	3.5 ± 0.7
MMSE [mean ± SD]*	21.7 ± 4.3	26.7 ± 2.4	30 ± 0
Education, years [mean ± SD]	16.5 ± 2.3	14.6 ± 2.1	19.0 ± 1.4
PES of FDG-ADCRP [mean ± SD]*	12.4 ± 8.8	6.0 ± 5.3	-5.7 ± 5.5
^{18}F-FDG uptake [mean ± SD]*	1.04 ± 0.09	1.10 ± 0.08	1.21 ± 0.03
Neuropathological diagnosis (N of subjects): Braak tangles stage	ADNC (24): 2-6 DLB (4): 2-4 FTLD-TDP (1): 1 HS (1): 2	ADNC (5): 1-5 AD (1): 5	ADNC (1): 0 PART (1): 2
Subjects with Aβ PET available			
Number of subjects with Aβ PET available	17	3	2
Age at scan [mean ± SD]	80.2 ± 8.6	83.9 ± 5.3	76.6 ± 15.2
Age at autopsy [mean ± SD]	82.6 ± 8.4	85.6 ± 5.5	79.5 ± 13.4
Scan-deaths, years [mean ± SD]	2.4 ± 1.1	1.7 ± 0.7	2.9 ± 1.8
MMSE [mean ± SD]*	23.4 ± 3.1	27.3 ± 2.0	30 ± 0
Education, years [mean ± SD]	17.2 ± 1.75	14.6 ± 3.0	19.0 ± 1.4
Aβ PET SUVr [mean ± SD]	1.43 ± 0.28	1.40 ± 0.20	1.43 ± 0.27
PES of Aβ-ADCRP [mean ± SD]	10.4 ± 24.6	3.5 ± 18.9	-9.9 ± 27.1
Neuropathological diagnosis (N of subjects): Thal amyloid phase	ADNC (13): 4-5 DLB (2): 1 FTLD-TDP (1): 1 HS (1): 1	ADNC (2): 4 AD (1): 5	ADNC (1): 1 PART (1): 0

AD, Alzheimer's disease, ADCRP, AD conversion-related pattern. SUVr, standardized uptake value ratio. ADNC, Alzheimer's disease neuropathological change. DLB, dementia with Lewy bodies. FTLD-TDP, frontotemporal lobar degeneration with TDP-43 inclusions. HS, hippocampal sclerosis. PART, primary age-related tauopathy. SD, standard deviation. All subjects were male. *significantly different between groups (ANOVA, $P < 0.01$).

TABLE 2. Diagnostic utility in detecting none-to-low vs. intermediate-to-high Alzheimer's disease neuropathological change.

		n	ROC AUC [±SE]	Cut-off	Sensitivity [95% CI]	Specificity [95% CI]
PCA-based	FDG	38	0.72 [±0.09]*	8.32	0.73 [0.52-0.88]	0.67 [0.35-0.90]
	FDG	22	0.80 [±0.10]*	7.39	0.79 [0.49-0.95]	0.75 [0.35-0.97]
	Aβ	22	0.95 [±0.05]**	-17.63	1.00 [0.77-1.00]	0.75 [0.35-0.97]
	Combined	22	0.98 [±0.02]**	-0.77	1.00 [0.77-1.00]	0.88 [0.47-1.00]
VOI-based	FDG	38	0.66 [±0.11]	1.09	0.73 [0.52-0.88]	0.67 [0.35-0.90]
	FDG	22	0.79 [±0.12]*	1.09	0.85 [0.57-0.98]	0.75 [0.35-0.97]
	Aβ	22	0.88 [±0.10]**	1.23	1.00 [0.77-1.00]	0.75 [0.35-0.97]
	Combined	22	0.90 [±0.08]**	-0.52	1.00 [0.77-1.00]	0.75 [0.35-0.97]

ROC AUC, area under the receiver operating characteristic curve. n, number of patients in the dataset. SE, standard error. CI, confidence interval. PCA, principal components analysis. VOI, volume of interest. Significance level vs. chance (ROC AUC = 0.50): ** $P < 0.001$; * $P < 0.05$.

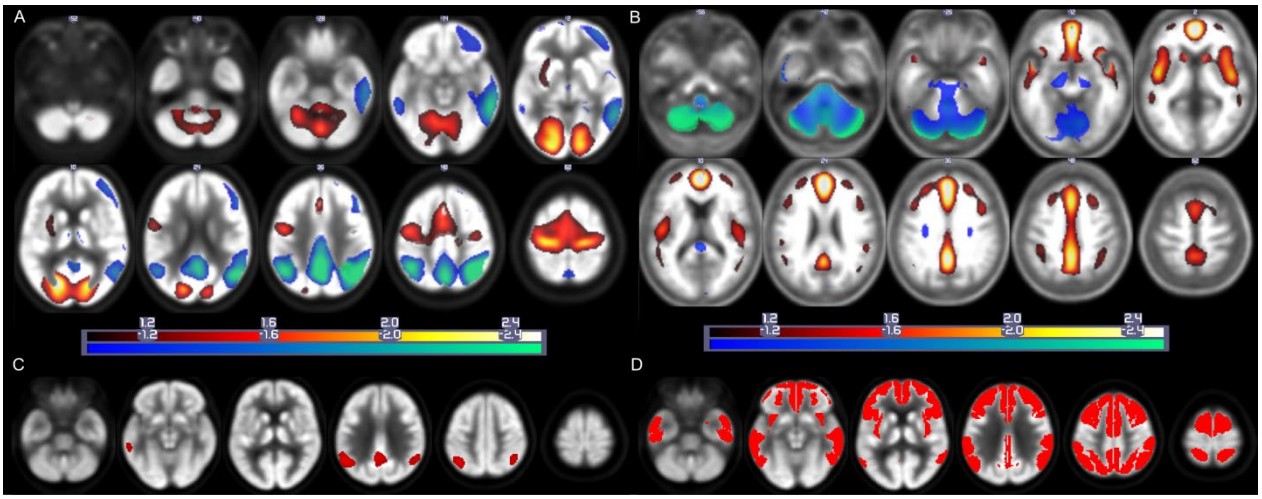

SUPPLEMENTAL FIGURE 1. Regions of highest weights in the Alzheimer's dementia conversion-related patterns (ADCRP). FDG-ADCRP overlaid on the ^{18}F-FDG PET template (A) and Aβ-ADCRP overlaid on the ^{18}F-AV-45 PET template (B). Binary regions of significant hypometabolism in MCI subjects who converted to AD compared to stable MCI subjects (obtained from a voxel-wise two-sampled t-test (1)) (C) and regions with the highest beta-amyloid burden in Alzheimer's disease (2) (D) used to extract VOI-based measures of ^{18}F-FDG and ^{18}F-AV-45, respectively.

References:

1. Blazhenets G, Ma Y, Sorensen A, et al. Principal components analysis of brain metabolism predicts development of Alzheimer dementia. J Nucl Med. 2019;60:837-843.

2. Frings L, Hellwig S, Spehl TS, et al. Asymmetries of amyloid-beta burden and neuronal dysfunction are positively correlated in Alzheimer's disease. Brain. 2015;138:3089-3099

SUPPLEMENTAL TABLE 1. Diagnosis, clinical and pathologic characteristics of cases incorrectly classified between none-to-low and intermediate-to-high ADNC stages by imaging biomarkers.

Clinical information						Pathology					Imaging							
Dx	MMSE	Scan-to-death, years		Age at PET, years		Primary Dx	Secondary Dx	Thal phase	Braak stage	ADNC	PES of FDG-ADCRP		PES of Aβ-ADCRP		Mean ^{18}F-FDG uptake		Mean ^{18}F-AV-45 SUVr	
^{18}F-FDG PET																		
		^{18}F-FDG PET	Aβ PET	^{18}F-FDG PET	Aβ PET													
ADD	24	2	2	79	79	HS	ADNC	1	2	Low	16.2	**FP**	-27.5	TN	1.09	TN	1.01	TN
MCI	25	2	2	88	88	ADNC	DLB	4	2	Low	3.3	TN	-17.6	TN	1.02	**FP**	1.16	TN
ADD	27	4	2	77	79	ADNC	DLB	5	2	Low	13.9	**FP**	9.9	**FP**	0.94	**FP**	1.39	**FP**
AD	18	5	NA	82	NA	DLB	ADNC	3	2	Low	13.5	**FP**	NA	-	1.01	**FP**	NA	-
AD	23	2	NA	82	NA	DLB	ADNC	4	2	Low	10.4	**FP**	NA	-	0.93	**FP**	NA	-
MCI	29	2	2	78	78	ADNC	-	4	3	Med	0.9	**FN**	18.7	TP	1.18	**FN**	1.55	TP
MCI	29	2	NA	87	NA	ADNC	SAL	3	3	Med	8.5	TP	NA	-	1.17	**FN**	NA	-
AD	26	4	4	87	87	ADNC	DLB	4	5	High	7.9	**FN**	20.6	TP	1.00	TN	1.39	TP
ADD	24	2	2	74	74	ADNC	DLB	5	5	High	6.2	**FN**	6.6	TP	1.01	TN	1.29	TP
MCI	28	1	1	85	85	AD	-	5	5	High	0.7	**FN**	9.5	TP	1.14	**FN**	1.49	TP
AD	22	8	NA	88	NA	ADNC	ARTAG	4	5	High	0.6	**FN**	NA	-	1.10	**FN**	NA	-
AD	24	6	NA	75	NA	ADNC	TDP-MTL	5	5	High	3.0	**FN**	NA	-	1.15	**FN**	NA	-
AD	17	4	NA	89	NA	ADNC	-	5	5	High	7.9	**FN**	NA	-	1.18	**FN**	NA	-
AD	19	2	NA	74	NA	ADNC	HS	4	5	High	15.7	TP	NA	-	1.10	**FN**	NA	-
Amyloid PET																		
		^{18}F-FDG PET	Aβ PET	^{18}F-FDG PET	Aβ PET													
CN	30	4	4	66	65	ADNC	-	1	1	Low	-9.6	TN	9.2	**FP**	1.23	TN	1.62	**FP**
ADD	27	4	2	77	79	ADNC	DLB	5	2	Low	13.9	**FP**	9.9	**FP**	0.94	**FP**	1.39	**FP**

Dx, diagnosis. MMSE, mini-mental state examination. ADNC, Alzheimer's disease neuropathological change. PES, pattern expression score. ADCRP, Alzheimer's disease dementia conversion-related pattern. SUVr, standardized uptake value ratio. AD, Alzheimer's disease. ADD, AD dementia. HS, hippocampal sclerosis. DLB, dementia with Lewy bodies. ARTAG, Aging-related tau astrogliopathy. TDP-MTL, TDP pathology circumscribed to the medial temporal lobe. SAL, subcortical arteriosclerotic leukoencephalopathy. MCI, mild cognitive impairment. CN, cognitively unimpaired. Med, intermediate. TN, true negative. TP, true positive. FN, false negative. FP, false positive.